Atmospheric Environment 105 (2015) 1–6

Contents lists available at ScienceDirect

Atmospheric Environment

journal homepage: www.elsevier.com/locate/atmosenv

Elemental composition and radical formation potency of PM10 at an urban background station in Germany in relation to origin of air masses

Bryan Hellack [a, *], Ulrich Quass [a], Henning Beuck [a], Gabriele Wick [b], Wilhelm Kuttler [c], Roel P.F. Schins [b], Thomas A.J. Kuhlbusch [a, d]

[a] Institute of Energy and Environmental Technology e.V. (IUTA), Bliersheimerstraße 58-60, 47229 Duisburg, Germany
[b] IUF – Leibniz Research Institute for Environmental Medicine, Auf'm Hennekamp 50, 40225 Duesseldorf, Germany
[c] University Duisburg-Essen, Faculty of Biology, Applied Climatology and Landscape Ecology, Schützenbahn 70, 45127 Essen, Germany
[d] Center for Nanointegration Duisburg-Essen (CENIDE), University Duisburg-Essen, Carl-Benz-Straße 199, 47057 Duisburg, Germany

HIGHLIGHTS

- PM10 radical formation potency is correlated to sources and origin of air mass.
- Source apportionment for the PM10 radical formation potency was performed.
- The PM10 radical formation potency was linked to the fossil fuel combustion factor.
- A seasonal trend for the PM10 radical formation potency was observed.

ARTICLE INFO

Article history:
Received 11 April 2014
Received in revised form
13 January 2015
Accepted 14 January 2015
Available online 15 January 2015

Keywords:
Particulate matter
EPR
DMPO
ROS
Hydroxyl radical
Source apportionment

ABSTRACT

At an urban background station in Mülheim-Styrum, North Rhine Westphalia, Germany, a set of 75 PM10 samples was collected over a one year period, followed by analyses for mass, chemical composition and hydroxyl radical (OH•) formation potency. Additionally, the origin of air masses for the sampling days was calculated by 48-h backward trajectories, subdivided into the four cardinal sectors. Significant lower PM10 mass concentrations were observed for summertime air masses from the west compared to the other seasons and cardinal sectors. For the OH• formation potency higher values were detected if air masses originate from east and south, thus predominantly being of continental origin. From the elevated OH• formation potencies in fall and winter a seasonal trend with low potencies in summers is assumed. Furthermore, source apportionment was performed by a positive matrix factor analysis, separating seven plausible factors which could be attributed to mineral dust, secondary nitrate, industry, non-exhaust traffic, fossil fuel combustion, marine aerosol and secondary aerosol factors. The intrinsic OH• formation potency was found to be associated mainly with the fossil fuel combustion factor (45%) and industry factor (22%).

1. Introduction

Epidemiological studies show associations between airborne particulate matter (PM) exposure and adverse health effects (Brook et al., 2010; Dockery et al., 1993). Furthermore, it is accepted by now that PM is capable of inducing toxicological responses in lung cells like increased production of inflammatory mediators or DNA strand breakage (Schaumann et al., 2004; Wessels et al., 2010). Such inflammatory and toxic effects of PM are typically observed in strong association with the physico-chemical properties of the particles

Abbreviations: AU, Arbitrary Units; DMPO, 5,5-dimethylpyrroline-N-oxide; DNA, Deoxyribonucleic Acid; EPR, Electron Paramagnetic Resonance; HYSPLIT, Hybrid Single Particle Lagrangian Integrated Trajectory; LOD, Limit of Detection; NOAA-NCEP, National Oceanic and Atmospheric Administration – National Weather Service's National Centres for Environmental Prediction; PM, Particulate Matter; PMF, Positive Matrix Factorization; ROS, Reactive Oxygen Species; SPSS, Statistical Package for the Social Sciences.

* Corresponding author. Institute of Energy and Environmental Technology e.V. (IUTA), Bliersheimerstraße 60, 47229 Duisburg, Germany.
E-mail address: hellack@iuta.de (B. Hellack).

http://dx.doi.org/10.1016/j.atmosenv.2015.01.033
1352-2310/

(Baulig et al., 2009; Gerlofs-Nijland et al., 2009; Knaapen et al., 2002; Schins et al., 2004). The generation of reactive oxygen species (ROS) by particles themselves or via the phagocytic cells of the immune system, leading to oxidative stress, is a linking and relevant parameter that can be associated to the PM hazard (Donaldson et al., 2004; Schaumann et al., 2004; Shi et al., 2006; Wessels et al., 2010). Thus, the measurement of the PM generated ROS capacity represents a promising indicator for particle-induced adverse health effects of ubiquitous particulate air pollutants (Ayres et al., 2008; Borm et al., 2007). PM composition is highly variable depending on its anthropogenic sources (e.g. traffic, industry) and/or natural sources (e.g. dust or sea spray) as well as on the weather conditions, season and other meteorological factors (Beverland et al., 2000; Borge et al., 2007; Putaud et al., 2010; Querol et al., 2004a, 2004b). The regional and supra regional influence is considered to mainly result from long-distance transport caused by large scale weather situations and atmospheric chemistry mechanisms. Consequently, also a variation of the PM10 related intrinsic ROS formation potency is expected. Therefore, in the present study we measured the hydroxyl radical (OH•) formation potency in PM10 filter extracts by a spin trap based electron paramagnetic resonance spectroscopy method. The hydroxyl radical (OH•) formation potency was then evaluated to its relation of origin of air mass, chemical content and potential PM sources by positive matrix factorization (PMF) analysis.

2. Materials and methods

2.1. Experimental design and method

We analysed PM10 mass, intrinsic OH• formation potency and several chemical compounds (Supplement data Table 1) of PM10 collected on quartz fibre filters at an urban background station in Styrum, North-Rhine Westphalia, Germany, over a one year period (2008–2009, Supplement data Table 2). The sampling method, location and chemical analysis are described in detail in Beuck et al. (2011). The OH• formation potency was measured using the EPR-technique following the method described in Hellack et al. (2014) and Shi et al. (2003). The principle of this ROS detection method is based on the trapping of PM elicited OH•, which is mainly generated via Fenton-type reaction in presence of H_2O_2. The potentially generated OH• are trapped by the also added spin trap DMPO (5,5-dimethylpyrroline-N-oxide). The results are expressed as concentration in OH· generation in arbitrary units per m^3 ambient air (a.u./m^3). Briefly, for the measurement the filters were placed in a vial covered with the reagents (DMPO, H_2O_2 and dH_2O) and agitated before being placed in a shaking water bath for 15 min incubation. After incubation the suspension was vortexed again, transferred into a glass capillary and measured with a MS-300 EPR spectrometer (Magnettech, Berlin, Germany).

2.2. Air mass and trajectory analysis

The HYSPLIT (Hybrid Single Particle Lagrangian Integrated Trajectory) dispersion model was used to calculate the origin of air masses by six hours stepwise 48-h backwards trajectories. Meteorological data were taken from the online available NOAA-NCEP (National Oceanic and Atmospheric Administration – National Weather Service's National Centres for Environmental Prediction). The trajectories of air masses were divided into four sectors according to main cardinal sectors, west (denoted seaside air masses, 225°–315°), east (continental air masses, 45°–135°), north (mixed – seaside dominated, 315°–45°) and south (mixed – continental dominated, 225 to 135°) (Fig. 1).

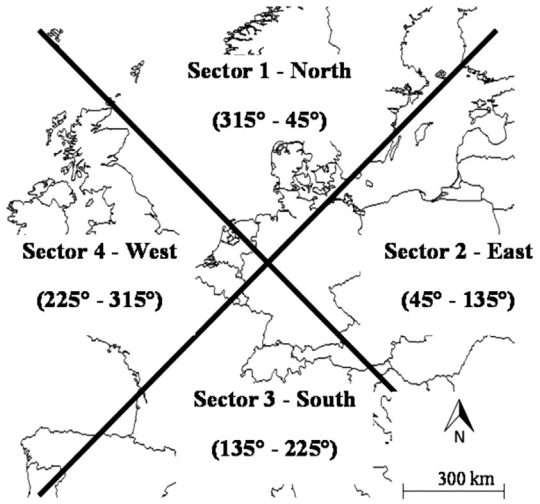

Fig. 1. Map showing the sampling location (crossing point = Styrum, Germany) and the sectors for the direction of air masses for the backward trajectory model: (1) North, (2) East, (3) South and (4) West.

2.3. Source apportionment

Source apportionment was performed by using the Positive Matrix Factorization (EPA PMF 3.0) with daily PM10 measurements including further chemical and OH• analysis data (Paatero, 1999; Viana et al., 2008). The PM composition data used were a subset of the data described in more detail by Beuck et al. (2011). Briefly, as input data for the concentration matrix all samples remaining positive after blank correction were used. Values becoming negative by blank correction were set to 0.00001 μg/m^3. The same was applied to values below 50% of the analytical detection limit (LOD, defined as 3-fold the standard deviation of the blank) in case of compounds with non-detectable filter blanks. Missing values were replaced by the respective compound averages. Measured element concentrations were transformed into probable related compounds, mostly oxides. Error estimates were assessed according the EPA PMF 3.0 User's Guide (Norris and Vedantham, 2007). Consequently, analytical uncertainties up to 30% and uncertainties for samples below LOD were assumed to be 5/6*LOD (Polissar et al., 1998). Species with a signal-to-noise (s/n) ratio between 0.2 and 2 were declared as weak variables. In addition to the chemical species, the measured PM masses were included into the model for the purpose of normalization. In order to avoid their influence on the model solution, their uncertainties were increased by a factor of four.

2.4. Statistical analysis

For statistical analyses, besides PMF, the SPSS (Statistical Package for the Social Sciences Version 11.0) program was used. Normal distribution of the data was checked via Kolmogorov–Smirnov Test; otherwise non parametric tests were applied.

3. Results

3.1. Mass, chemical composition and intrinsic OH· formation potency analyses related to the origin of air masses by backward trajectory model

For the 75 analysis days 33% and 32% of the air masses originated from sector 2 (East) and sector 4 (West), respectively. Both other sectors had significant lower values (16%, North and 5%,

South), while 14% of the trajectories could not be clearly assigned to one of these four sectors (way of trajectory ≤85% within a specific sector) and have thus not been considered in the further analysis (for sector). The dominance of west and east direction was due to pre-selection of samples for analysis, since the sampling campaign originally was designed to assess the influence of natural sources on PM10 (Beuck et al., 2011). An overview of the detected OH• values is given in Table 1.

When looking to sectoral differences PM10 mass showed significant lower values for the west sector compared to the south and east sector on the level of $p < 0.01$ (Mann–Whitney-U test) (Table 2). Due to the geographical position the sampling station it is influenced by the interaction of Icelandic Lows (Cyclones) and Azores High (Anticyclones) characterized by turbulent air masses leading to dilution of PM concentrations. For the intrinsic OH· formation potency significant higher values for the east and south compared to north and west became obvious using the Kruskal & Wallis and Mann–Whitney-U test (Table 2). The elemental composition of PM10 varied as expected among sectors and seasons. Significant sector differences of the elemental composition were seen for the parameters EC, OM, NH_4^+, Cl^-, Na^{2+}, Mg^{2+}, Al_2O_3, Ca, SiO_2, Sb_2O_3, MoS_2, CuO, As_2O_3 and Cr_2O (Mann–Whitney-U test). The parameters EC, OM, Al_2O_3, Ca, SiO_2, Sb_2O_3, MoS_2, CuO, As_2O_3 and Cr_2O show high contribution for the east and south sectors, thus being continental influenced, whereas the parameters NH_4^+, Cl^-, Na^{2+} and Mg^{2+} (seaside influenced parameters) show the lowest contribution to the east and south sectors (Supplement data Table 3).

Among others, a correlation analysis was performed using the Kendall–Tau test, showing significant but weak ($R = 0.21$) correlation ($p \leq 0.05$) between intrinsic OH· formation potency and PM10 mass. Further, almost well known inter-element correlations because of similar sources (e.g. Fe and Cu) are shown in Supplement Table 4 and will be also indirectly reflected by the PMF analysis later on by their affiliation to the different factors.

Analysis of the seasonal pattern (Kruskal & Wallis and Mann–Whitney-U test, $p \leq 0.05$) indicates lower, but not significant, PM10 concentrations for the summertime compared to spring and winter. For spring nine of the in sum 19 trajectories came from the north whereas for the winter similar to the west six trajectories came from the east. The lower OH• values in the summer might be caused by slightly dominance of numbers of western trajectories (Table 3).

For OH· formation potency significant differences were observed with lower concentrations for spring and summer compared to higher values in fall and winter (Fig. 2).

Like for the seasonal trend, significant wind direction sector differences ($p \leq 0.01$) were detected for the OH• formation potency showing significant higher values for the east and south sector. For PM only the west sector showed significant differences ($p \leq 0.01$) with lower values than for the other sectors (Fig. 3).

Table 1
Statistical description of the intrinsic OH· formation potency (a.u./m³).

	Season	Sector
	n = 75	n = 65
Mean	38.0	37.8
95% Confidence interval		
Lower limit	34.2	33.6
Upper limit	41.7	41.9
5% Trimmed mean	37.3	37.1
Median	35.1	31.4
Variance	265.6	280.9
SD	16.3	16.8
Minimum	13.5	13.5
Maximum	76.4	76.4
Width	62.9	62.9
Interquartile range	28.3	28.5
Standard error	1.9	2.1

Table 2
Overview of the mean PM10 mass and intrinsic OH· formation potency related to the origin of air masses by trajectory modelling.

	Trajectories			PM10 (µg/m³)		OH• (a.u./m³)	
	N	N of days	(%)	Mean	SD	Mean	SD
North	48	12	16	33.7	15.0	29.4	14.9
East	100	25	33	**36.0**	13.0	*44.3*	15.8
South	16	4	5	*35.2*	9.0	**48.7**	11.4
West	96	24	32	24.7	10.0	33.3	15.7
Indefinable	40	10	14	34.2	12.8	39.4	13.0
Sum	300	75	100	32.8	13.8	38.0	16.2

In **bold**: highest value; in *italic*: second highest value (without indefinable class).

Table 3
Seasonality of the backward trajectories.

	North	East	South	West	Sum
Spring	6	9	–	4	19
Summer	3	4	–	9	16
Fall	–	6	2	5	13
Winter	3	6	2	6	17
Sum	12	25	4	24	65

3.2. Identification and contribution of sources

The PMF (EPA PMF 3.0) identified seven plausible factors that were classified based on former source apportionment studies (Bruinen de Bruin et al., 2006; Limbeck et al., 2009; Schwela et al., 2002; Viana et al., 2008). An overview of the evaluated factors and their probable sources/processes (as factor name) is given in Table 4. Around 19% of the species were contributed to the mineral dust and non-exhaust traffic factor, whereas the other five factors revealed similar contributions of the species of 11%–14%. The relatively high contribution of the mineral dust factor might be caused by the pre-selection of samples for analysis, since the sampling campaign originally was designed to assess the influence

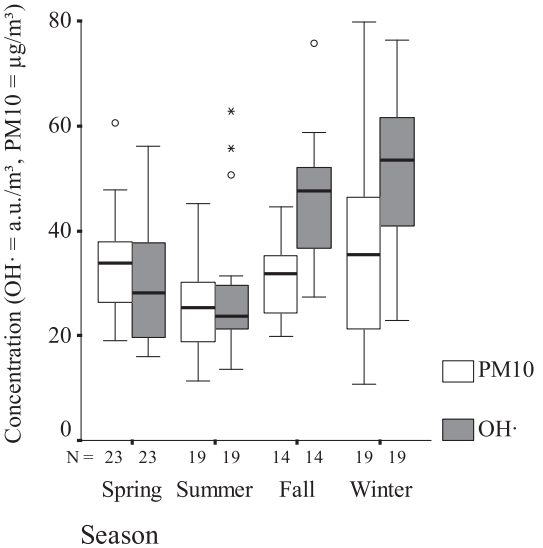

Fig. 2. Seasonal variation of OH• (a.u./m³) and PM10 (µg/m³) concentration; o = outlier (1.5–3.0 inter quartile range, IQR); * = extreme value (>3.0, IQR).

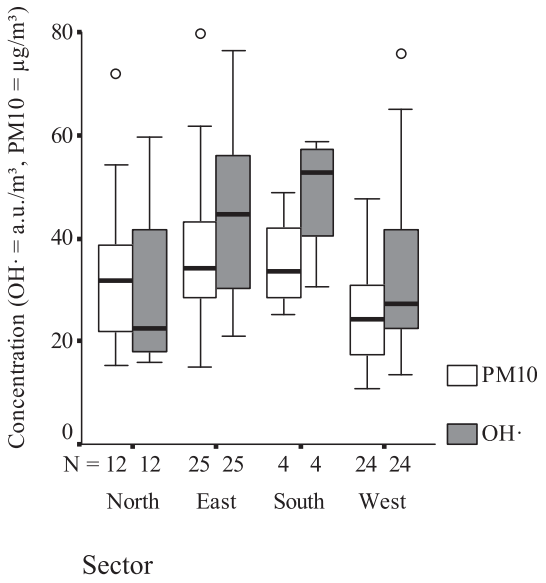

Fig. 3. Variation of OH• formation potency (a.u./m^3) and PM10 (µg/m^3) concentration for the four wind direction sectors; o = outlier (1.5–3.0 inter quartile range, IQR); * = extreme value (>3.0, IQR).

of natural sources on PM10 (Beuck et al., 2011). Another reason could be mineral dust long distance transport as well shown by the relatively high OM contribution to this factor. The factor profiles and element classification to the factors are shown in Table 5. For this PMF result, the predicted PM10 mass reproduces sufficiently the measured PM10 mass and accounts for most of the variation in the PM masses (slope: 0.94; offset: 1414 ng/m^3, R^2 = 0.93). Furthermore, the modelled factors do not correlate with each other. The regression coefficients between the factors are below 0.15, indicating that all factors are sufficiently independent. FPEAK value was kept at zero. These results show a good agreement between Q(true) and Q(robust) and the scaled residuals are normally distributed (Table 5).

In order to identify the contribution of the parameters to the different factors the PMF was done with and without intrinsic OH• formation potency to check whether or not this parameter has an influence on the factor analysis. No significant differences for the factor composition and contribution were detected.

All factors, except factor 2, were common showing high factor contribution for at least two variables for each factor (Table 6). Factor 1 was declared as the mineral dust factor associated to Al_2O_3, $CaCO_3$, Ca^{2+}, SiO_2, TiO_2 and to V_2O_5. Factor 2 is a single factor due mainly to the contribution of nitrate and called the secondary nitrate factor. However, it was also associated to ammonium and chloride. Factor 3 is an industry/burning emission factor dominated by ZnO and PbO in addition to EC, OM, K^+ and CdO. The factor 4, a non-exhaust traffic factor, was mainly due to Fe_2O_3, Sb_2S_3, MoS_2, CrO_2 and NiO. Factor 5 was strongly correlated with K^+, As_2O_3, CdO, EC, OM and OH•, which comprises markers for fossil fuel combustion. Factor 6 was the marine aerosol factor with the highest contribution from Cl^- Mg^{2+} and Na^{2+}. Finally factor 7 was the secondary sulphate factor comprising high shares of sulphate and NH_4^+, as well as a moderate amount of nitrate.

To sum up main contribution from OH formation potency was contributed by factor 5, the fossil fuel combustion.

Table 4
Mean contribution of the via PMF calculated factors and their probable source processes as factor names.

Factor N°	Factor name	Contribution of the species (%)
1	Mineral Dust	19
2	Secondary Nitrate	11
3	Industry	11
4	Non Exhaust Traffic	19
5	Fossil Fuel Combustion	14
6	Marine Aerosol	12
7	Secondary Sulphate	14

Table 5
Overview of the Qtrue and QRobust values.

Run	Q(Robust)	Q(True)
1	586.401	586.391
2	589.084	589.067
3	586.332	586.324
4	586.660	586.646
5	586.351	586.345
6	592.243	592.191
7	586.262	586.253
8	612.535	612.514
9	592.300	592.236
10	587.936	587.923
11	589.629	589.598
12	586.412	586.403
13	612.635	612.608
14	590.831	590.798
15	589.566	589.529
16	590.749	590.732
17	593.226	593.157
18	586.406	586.400
19	589.543	589.509
20	589.566	589.531

3.3. Sector differences due to sources and season

The PMF-derived factors were analysed again for their dependency on wind sector and season. For the marine aerosol factor (6) significant differences became obvious with higher contributions from western- and northern derived air masses compared to air masses from the east or south (Kruskal & Wallis and Mann–Whitney-U tests, $p \leq 0.05$). In contrast the fossil fuel combustion factor (5) as well as the mineral dust factor (1) revealed significant lower contributions from the western originated air masses compared to eastern air masses. In Table 7 these significant differences of the mean value to the sectors are marked with indication of the sector that differs. Due to the geographical position of the sampling location this results are logic. Long distance PM transport might lead to enlarged contribution of the mineral dust and fossil fuel combustion from continental, eastern European areas. The eastern driven fossil fuel combustion factor could be additionally due to emissions from the industrial Ruhr Area.

Additionally, seasonal differences were analysed. The mineral dust, secondary nitrate, industry and fossil fuel combustion factors showed significant differences ($p < 0.05$, Kruskal & Wallis and Mann–Whitney-U test) between different seasons. The mineral dust factor showed lowest contributions in the wintertime, compared to spring- and summertime values. The secondary nitrate factor showed lowest contribution in the summertime, while e.g. the highest contributions of the fossil fuel combustion factor were detected in the wintertime. These seasonality of the factors are explainable by the geographical position and its resulting meteorology leading e.g. to higher fossil fuel combustion in wintertime in western and eastern Europe. In Table 8 these significant differences of the mean value of the season are marked with specification of the sector that differs.

In sum for our sampling location, due the geographical position, eastern driven air masses influenced by fossil fuel combustion in wintertime do have highest OH• formation potency.

Table 6
Overview of the factor profiles and parameter contribution to the factors expressed as total concentration of species in % (right side is the prosecution of the left side).

Factor	Concentration of species total in %							Factor	Concentration of species total in %						
	1	2	3	4	5	6	7		1	2	3	4	5	6	7
EC	10.1	4.1	*24*	16.5	**34**	–	11.4	Fe_2O_3	18.7	*19.5*	3.3	**47.7**	1.8	8.8	0.2
OM	22.1	–	*23.8*	13.2	**28**	4	9.1	MnO_2	–	10.9	3.2	**51**	–	7.9	*27*
NO_3^-	–	**69.5**	–	–	–	11.9	*18.5*	ZnO	9.7	15	**35.5**	*29.9*	1.6	8.2	–
SO_4^{2-}	2.1		17	1	*20.1*	3.1	**56.7**	Sb_2S_3	14.4	20	4.1	**31**	*27.2*	3.4	–
NH_4^+	–	*29.2*	3.4		10.5	0.3	**56.6**	MoS_2	15.6	8	–	**42.5**	*22.5*	2.5	8.8
Cl^-	–	*18*	–	5.3	11.6	**65.1**	–	CuO	*25.5*	19.6	0.5	**43.4**	11	–	–
Na^+	2.2	–	–	–	*14.6*	**71.7**	11.5	As_2O_3	–	9.5	–	20.6	**45.4**	2.9	*21.5*
Mg^{2+}	*21.8*	1.3	7.5	–	–	**52.5**	17	CdO	3.8	9.6	*27.8*	11.1	**29.9**	6.3	11.4
Al_2O_3	**54.1**	4.5	1.5	*20.8*	9.4	3	6.6	Cr_2O_3	4.6	–	3.9	**77.8**	–	–	*13.7*
$CaCO_3$	**43.8**	11.8	–	*38.3*	–	6.1	–	NiO	*12.9*	5.8	8.5	**43.5**	5.8	10.7	12.8
Ca^{2+}	**53.2**	3.8	4.4	*15.4*	6.6	9.9	6.8	PbO	9	2.2	**52.1**	6.6	5	11.4	*13.6*
SiO_2	**70.9**	–	–	7	*11.9*	3.6	6.6	V_2O_5	**36.6**	5	25.6	–	–	2.4	*30.4*
K^+	–	4	*34.7*	2.6	**35.2**	11.4	12.1	PM10	13.4	*17.6*	11.3	8.6	15.3	7.2	**26.7**
TiO_2	**59.8**	6.5	–	–	10.1	7.4	*16.2*	OH•	15.1	–	*21.1*	11.3	**44.8**	7.6	–

The highest value is shown in **bold** and the second highest value in *italic* showing the factor affiliation.

4. Discussion

Similar to the variation of PM10, the OH• formation potency is also expected to vary. So far only a few studies dealt with OH• formation potency of PM and demonstrated a variation depending on site, particle composition and sources (Boogaard et al., 2013; Janssen et al., 2013; Kunzli et al., 2006; Nawrot et al., 2009; Orru et al., 2010; Shi et al., 2006; Wessels et al., 2010; Yang et al., 2014). Furthermore, the intrinsic OH• formation potency was shown to be a parameter not or just weakly correlated to the PM mass (Janssen et al., 2013; Yang et al., 2014). However the results of this study are not directly comparable as not always the same ROS detection method was used. So far several promising detection methods are available (Borm et al., 2007), whereas in this study the EPR approach was applied because of already shown correlation of this method to adverse health effects for instance with DNA oxidation and release of the inflammatory marker interleukin-8 in human lung cells (Wessels et al., 2010) as well as with markers of lung inflammation in humans (Schaumann et al., 2004). This indicates that measurement of the Fenton-like mediated oxidant generating properties is a sensitive method to estimate the toxic potency of PM. However, the applied assay should be seen as one out of a number of "artificial" approaches to determine the oxidative properties of PM. In the current method, H_2O_2 is added to the particle suspensions to more or less reflect the reducing environment residing within the respiratory tract. Other approaches determine e.g. the ability of PM to deplete antioxidants like glutathione or ascorbate in lung-lining resembling fluids or that quantify quinone cycling radials from the organic components within the PM mixture (Borm et al., 2007). Importantly, the presently applied ESR method has been found also to correlate well with antioxidant depletion methods that use glutathione and ascorbate (Kuenzli et al., 2006).

As PM2.5 is a part of PM10 and assuming that the OH• triggering particles, especially transition metals caused by abrasion and combustion processes (Wessels et al., 2010), are predominantly in the smaller fraction, our results become comparable to a former study by Orru et al. (2010). In this study, similar to ours, the variation of PM2.5 OH• formation potency in relation to source, origin of air masses and season in Tartu, Estonia, was investigated. Higher PM2.5 content, in our case PM10, and a higher oxidative capacity could be shown if air masses originated from the east in Tartu as well in Styrum. Furthermore in Tartu the factor analysis revealed the highest OH• contribution for the industry and fossil fuel combustion factor. The east air masses were dominated, compared to the other sectors, by fossil fuel combustion assuming to contain notable concentrations of polycyclic aromatic hydrocarbons (PAH) being reactive, either alone or together with transition metals in the formation of OH• (de Kok et al., 2005; Ntziachristos et al., 2007). However the PAH could just be a proxy for other (unknown) sources that drive the H_2O_2 dependent OH formation in the EPR method. Coining this to our study, the eastern driven fossil fuel combustion factor could be due to emissions from the Ruhr Area, which is the largest and densest German agglomeration of industry and traffic as well from eastern European countries. Additional contribution might be obtained from the eastern European countries via wood fire and/or wooden and coal heating processes. The seasonal trends of lower OH• formation potency values at summertime were in contrast to the results of Orru et al. (2010) who found relatively higher values in spring and summer caused by relatively high ozone concentrations at their measurement campaign.

Table 7
Mean factor contributions of PM10 in % of total modelled PM10 with indication of significant sector differences.

Factor	N	Mineral dust	Fossil fuel combustion	Marine aerosol
North (N)	12	24^{E}	18^{E}	$39^{E,S}$
East (E)	25	$\mathbf{42^{N,S,W}}$	$36^{N,W}$	$\mathit{1}^{N,S,W}$
South (S)	4	31^{E}	36	$9^{N,W,E}$
West (W)	24	21^{E}	11^{E}	$51^{S,E}$

^{N} – mean value different from North, ^{E} – mean value different from East, ^{S} – mean value different from South, ^{W} – mean value different from West (for all $p \leq 0.05$); in **bold** (highest values) and in *italic* (lowest values) highest significant differences are marked.

Table 8
Mean factor contributions of PM10 in % of total modelled PM10 with indication of significant seasonal differences.

Factor	N	Mineral dust	Secondary nitrate	Industry	Fossil fuel combustion
Spring (S)	23	34^{W}	31^{Su}	15^{F}	15^{W}
Summer (Su)	19	29^{W}	$\mathit{6}^{S,W,F}$	22^{F}	$9^{F,W}$
Fall (F)	14	34^{W}	31^{Su}	$\mathbf{38^{S,Su,F}}$	$23^{Su,W}$
Winter (W)	19	$\mathit{4}^{S,Su,F}$	32^{Su}	26^{F}	$\mathbf{53^{S,Su,F}}$

^{S} – mean value different from Spring, ^{Su} – mean value different from Summer, ^{F} – mean value different from Fall, ^{W} – mean value different from Winter (for all $p \leq 0.05$); in **bold** (highest values) and in *italic* (lowest values), the highest significant differences are marked.

5. Conclusion

This study shows that the dependence of the elemental composition of PM10 at this urban background station in terms of the intrinsic OH• formation potency is related to the PM source and origin of air masses. The highest contribution to the intrinsic OH• formation potency was correlated to the factor of fossil fuel combustion and to the industry factor. The lowest influence was detected for the air masses from the west and dominated by marine aerosols. These results show that the influence of the air mass transport direction as already known for PM values also holds for the OH• generation potency.

Since OH· generation potency is not or just weakly correlated with PM mass and the potential PM mass based induced toxicity is source dependent the measure of the PM elicit OH• formation potency serves as a complementary measure to PM mass which might be applicable for environmental monitoring and also useful for epidemiological studies addressing PM related health effects.

Acknowledgement

We gratefully acknowledge the Landesamt für Natur, Umwelt und Verbraucherschutz North Rhine-Westphalia (LANUV NRW) for its support, and permit to use the chemical composition analysis data and re-analyse the filter samples.

Appendix A. Supplementary data

Supplementary data related to this article can be found at http://dx.doi.org/10.1016/j.atmosenv.2015.01.033.

References

Ayres, J.G., Borm, P.A., Cassee, F.R., Castranova, V., Donaldson, K., Ghio, A., et al., 2008. Evaluating the toxicity of airborne particulate matter and nanoparticles by measuring oxidative stress potential – a workshop report and consensus statement. Inhal. Toxicol. 20, 75–99.

Baulig, A., Singh, S., Marchand, A., Schins, R., Barouki, R., Garlatti, Ml, et al., 2009. Role of Paris PM2.5 components in the pro-inflammatory response induced in airway epithelial cells. Toxicology 261, 126–135.

Beuck, H., Quass, U., Klemm, O., Kuhlbusch, T.A.J., 2011. Assessment of sea salt and mineral dust contributions to PM10 in NW Germany using tracer models and positive matrix factorization. Atmos. Environ. 45, 5813–5821.

Beverland, I.J., Tunes, T., Sozanska, M., Elton, R.A., Agius, R.M., Heal, M.R., 2000. Effect of long-range transport on local PM 10 concentrations in the UK. Int. J. Environ. Health Res. 10, 229–238.

Boogaard, H., Janssen, N.A., Fischer, P.H., Kos, G.P., Weijers, E.P., Cassee, F.R., et al., 2013. Contrasts in oxidative potential and other particulate matter characteristics collected near major streets and background locations. Environ. Health Perspect. 120, 185–191.

Borge, R., Lumbreras, J., Vardoulakis, S., Kassomenos, P., RodrÃ-guez, E., 2007. Analysis of long-range transport influences on urban PM10 using two-stage atmospheric trajectory clusters. Atmos. Environ. 41, 4434–4450.

Borm, P.J.A., Kelly, F., Kunzli, N., Schins, R.P.F., Donaldson, K., 2007. Oxidant generation by particulate matter: from biologically effective dose to a promising, novel metric. Occup. Environ. Med. 64, 73–74.

Brook, R.D., Rajagopalan, S., Pope 3rd, C.A., Brook, J.R., Bhatnagar, A., Diez-Roux, A.V., et al., 2010. Particulate matter air pollution and cardiovascular disease: an update to the scientific statement from the American Heart Association. Circulation 121, 2331–2378.

Bruinen de Bruin, Y., Koistinen, K., Yli-Tuomi, T., Kephalopoulos, S., Jantunen, M., 2006. Source Apportionment Techniques and Marker Substances Available for Identification of Personal Exposure, Indoor and Outdoor Sources of Chemicals. Joint Research Center JRC. ISPRA.

de Kok, T.M., Hogervorst, J.G., Briede, J.J., van Herwijnen, M.H., Maas, L.M., Moonen, E.J., et al., 2005. Genotoxicity and physicochemical characteristics of traffic-related ambient particulate matter. Environ. Mol. Mutagen 46, 71–80.

Dockery, D.W., Pope 3rd, C.A., Xu, X., Spengler, J.D., Ware, J.H., Fay, M.E., et al., 1993. An association between air pollution and mortality in six U.S. cities. N. Engl. J. Med. 329, 1753–1759.

Donaldson, K., Jimenez, L.A., Rahman, I., Faux, S.P., MacNee, W., Gilmour, P.S., et al., 2004. Respiratory health effects of ambient air pollution particles: the role of reactive species. In: Vallyathan, V., Shi, X., Castranova, V. (Eds.), Oxygen/Nitrogen Radicals: Lung Injury and Disease 187Marcel Dekker, New York.

Gerlofs-Nijland, M.E., Rummelhard, M., Boere, A.J.F., Leseman, D.L.A.C., Duffin, R., Schins, R.P.F., et al., 2009. Particle induced toxicity in relation to transition metal and polycyclic aromatic hydrocarbon contents. Environ. Sci. Technol. 43, 4729–4736.

Hellack, B., Yang, A., Cassee, F.R., Janssen, N.A.H., Schins, R.P.F., Kuhlbusch, T.A.J., 2014. Intrinsic hydroxyl radical generation measurements directly from sampled filters as a metric for the oxidative potential of ambient particulate matter. J. Aerosol Sci. 72, 47–55.

Janssen, N.A., Yang, A., Strak, M., Steenhof, M., Hellack, B., Gerlofs-Nijland, M.E., et al., 2013. Oxidative potential of particulate matter collected at sites with different source characteristics. Sci. Total Environ. 472C, 572–581.

Knaapen, A., Shi, T., Borm, P.A., Schins, R.F., 2002. Soluble metals as well as the insoluble particle fraction are involved in cellular DNA damage induced by particulate matter. Mol. Cell. Biochem. 234–235, 317–326.

Kuenzli, N., Mudway, I.S., Gotschi, T., Shi, T., Kelly, F.J., Cook, S., et al., 2006. Comparison of oxidative properties, light absorbance, total and elemental mass concentration of ambient PM2.5 collected at 20 European sites. Environ. Health Perspect. 114, 684–690.

Limbeck, A., Handler, M., Puls, C., Zbiral, J., Bauer, H., Puxbaum, H., 2009. Impact of mineral components and selected trace metals on ambient PM10 concentrations. Atmos. Environ. 43, 530–538.

Nawrot, S.T., Kuenzli, N., Sunyer, J., Shi, T., Moreno, T., Viana, M., et al., 2009. Oxidative properties of ambient PM2.5 and elemental composition: heterogeneous associations in 19 European cities. Atmos. Environ. 43, 4595–4602.

Norris, G.A., Vedantham, R., 2007. EPA Positive Matrix Factorization (PMF) 3.0 Fundamentals & User Guide. U. S. Environmental Protection Agency, National Exposure Research Laboratory, Research Triangle Park, NC.

Ntziachristos, L., Froines, J.R., Cho, A.K., Sioutas, C., 2007. Relationship between redox activity and chemical speciation of size-fractionated particulate matter. Part Fibre Toxicol. 4, 5.

Orru, H., Kimmel, V., Kikas, U., Soon, A., Kunzli, N., Schins, R.P., et al., 2010. Elemental composition and oxidative properties of PM(2.5) in Estonia in relation to origin of air masses – results from the ECRHS II in Tartu. Sci. Total Environ. 408, 1515–1522.

Paatero, P., 1999. The multilinear Engine: a table-driven, least squares program for solving multilinear problems, including the n-way parallel factor analysis model. J. Comput. Graph. Stat. 8, 854–888.

Polissar, A.V., Hopke, P.K., Paatero, P., Malm, W.C., Sisler, J.F., 1998. Atmospheric aerosol over Alaska: 2. Elemental composition and sources. J. Geophys. Res. Atmos. 103, 19045–19057.

Putaud, J.P., Van Dingenen, R., Alastuey, A., Bauer, H., Birmili, W., Cyrys, J., et al., 2010. A European aerosol phenomenology 3: physical and chemical characteristics of particulate matter from 60 rural, urban, and kerbside sites across Europe. Atmos. Environ. 44, 1308–1320.

Querol, X., Alastuey, A., Ruiz, C.R., ArtiÃ±ano, B., Hansson, H.C., Harrison, R.M., et al., 2004a. Speciation and origin of PM10 and PM2.5 in selected European cities. Atmos. Environ. 38, 6547–6555.

Querol, X., Alastuey, A., Viana, M.M., Rodriguez, S., ArtiÃ±ano, B., Salvador, P., et al., 2004b. Speciation and origin of PM10 and PM2.5 in Spain. J. Aerosol Sci. 35, 1151–1172.

Schaumann, F., Borm, P.J., Herbrich, A., Knoch, J., Pitz, M., Schins, R.P., et al., 2004. Metal-rich ambient particles (particulate matter 2.5) cause airway inflammation in healthy subjects. Am. J. Respir. Crit. Care Med. 170, 898–903.

Schins, R.P., Lightbody, J.H., Borm, P.J., Shi, T., Donaldson, K., Stone, V., 2004. Inflammatory effects of coarse and fine particulate matter in relation to chemical and biological constituents. Toxicol. Appl. Pharmacol. 195, 1–11.

Schwela, D., Morawska, L., Kotzias, D., 2002. Guidelines for Concentration and Exposure Response Measurement of Fine and Ulrafine Particulate Matter for Use in Epidemiological Studies. World Health Organization, Geneva, p. 185.

Shi, T., Duffin, R., Borm, P.J.A., Li, H., Weishaupt, C., Schins, R.P.F., 2006. Hydroxyl-radical-dependent DNA damage by ambient particulate matter from contrasting sampling locations. Environ. Res. 101, 18–24.

Shi, T., Schins, R.P.F., Knaapen, A.M., Kuhlbusch, T., Pitz, M., Heinrich, J., et al., 2003. Hydroxyl radical generation by electron paramagnetic resonance as a new method to monitor ambient particulate matter composition. J. Environ. Monit. 5, 550–556.

Viana, M., Kuhlbusch, T.A.J., Querol, X., Alastuey, A., Harrison, R.M., Hopke, P.K., et al., 2008. Source apportionment of particulate matter in Europe: a review of methods and results. J. Aerosol Sci. 39, 827–849.

Wessels, A., Birmili, W., Albrecht, C., Hellack, B., Jermann, E., Wick, G., et al., 2010. Oxidant generation and toxicity of size-fractionated ambient particles in human lung epithelial cells. Environ. Sci. Technol. 44, 3539–3545.

Yang, A., Jedynska, A., Hellack, B., Kooter, I., Hoek, G., Brunekreef, B., et al., 2014. Measurement of the oxidative potential of PM2.5 and its constituents: the effect of extraction solvent and filter type. Atmos. Environ. 83, 35–42.